XII International Conference on Computational Plasticity. Fundamentals and Applications
COMPLAS XII
E. Oñate, D.R.J. Owen, D. Peric and B. Suárez(Eds)

A NEW 3D-BEAM FINITE ELEMENT INCLUDING NON-UNIFORM TORSION WITH THE SECONDARY TORSION MOMENT DEFORMATION EFFECT

JUSTIN MURIN*, MEHDI AMINBAGHAI, VLADIMIR KUTIS* AND HERBERT A. MANG****

* Department of Applied Mechanics and Mechatronics, IPEAE FEI STU in Bratislava, Ilkovičova 3, 812 19 Bratislava, Slovakia
Email: justin.murin@stuba.sk, vladimir.kutis@stuba.sk, mehdi.aminbaghai@tuwien.ac.at, http://aladin.elf.stuba.sk/Katedry/KMECH/

**Institute for Mechanics of Materials and Structures
Vienna University of Technology Karlsplatz 13, A-1040 Vienna, Austria
email: mehdi.aminbaghai@tuwien.ac.at, http://www.imws.tuwien.ac.at

Key words: Non-uniform Torsion of Open and Closed Cross Sections, 3D Timoshenko Beam Finite Element, Secondary Torsion Moment Deformation Effect.

Abstract. In this paper, a new 3D Timoshenko linear-elastic beam finite element including warping torsion will be presented which is suitable for analysis of spatial structures consisting of constant open and hollow structural section (HSS) beams. The analogy between the 2nd-order beam theory (with axial tension) and torsion (including warping) was used for the formulation of the equations for non-uniform torsion. The secondary torsional moment deformation effect and the shear force effect are included into the local beam finite element stiffness matrix. The warping part of the first derivative of the twist angle was considered as an additional degree of freedom at the finite element nodes. This degree of freedom represents a part of the twist angle curvature caused by the bimoment. Results of the numerical experiments are discussed, compared and evaluated. The importance of the inclusion of warping in stress-deformation analyses of closed-section beams is demostrated.

1 INTRODUCTION

In stress and deformation analyses of thin-walled structures subjected to torsion, warping effects must be considered. They occur mainly at the points of action of concentrated torsion moments (except for free ends) and at sections with warping restraints. Special theories of torsion with warping, usually referred to as non-uniform torsion or warping torsion, have been used to solve such problems analytically (e.g. [1]). The analogy between the 2nd-order beam theory with axial tension and torsion including warping is also very often used (e.g. [2], [3]). However, it is worth of note that in the literature and in engineering practice, as well as in the Eurocode 3 [4] and Eurocode 9 [5] guidelines, a significant effect of warping is assumed to occur in open cross-sections only. Warping-based stresses and deformations in hollow sections are assumed to be insignificant, and have, therefore, been neglected.

According to the above aformentioned theory of torsion of open cross-sections including warping and according the mentioned analogy, special beam finite elements were designed and implemented into finite element codes (e.g. [6], [7]). The warping effect was included through an additional degree of freedom at each nodal point - the first derivative of the angle of twist of the cross-section of the beam. Important progress in the solution of torsion with warping is documented in [8] and [9] where a combination of the boundary and the finite element method (BEM and FEM) was used that allows a warping analysis for composite beams with the longitudinally varying cross-section.

However, recent theoretical results have shown that the effect of warping must also be considered for the case of closed-section beams [10]. For the investigated prismatic beams, the analogy between the warping torsion and the 2nd-order beam theory has to be used. This approach was implemented into the computer code IQ-100 [13]. However the analogy does not hold for non-prismatic beams [11].

Based on recent research concerning the aforementioned analogy, represented in [10], [11], [12] and [14], the local stiffness relation of a new two-node finite element for torsion including warping of straight beam structures was derived [15]. The warping part of the first derivative of the twist angle was considered as the additional degree of freedom for the end points of the element. This degree of freedom can be regarded as part of the curvature of the twist angle, caused by the bimoment. This new finite element can be used in non-uniform torsion analyses of both open and HSS straight beams. In [16], the BEM was applied to non-uniform torsion analysis of simply or multiply connected bars with doubly symmetrical arbitrary constant cross-sections, taking into account the effect of secondary torsional moment deformations. Herewith, a necessity of the non-uniform torsion effect consideration in the analysis of HSS beam was confirmed. Finally, in [17], a BEM was applied for the inelastic non-uniform torsion analysis of simply or multiply connected prismatic bars with arbitrarily shaped doubly symmetric cross section, where the secondary torsion moment deformation effect was included.

In this paper, which is an extension of the [15], a new Timoshenko 3D beam finite (W-beam) element for structural analysis of spatial beam structures will be presented. The classic 12x12 local stiffness matrix of the 3D beam finite element will be extended to 14x14. The effect of the deformations due to secondary torsional moments and the influence of shear forces are considered. The warping part of the first derivative of the twist angle is taken as the additional nodal degree of freedom.

By the transformation of the local finite element matrix and vectors the global finite element equation was obtained. The derived finite element equations were implemented into the computer program and numerical experiment was carried out. Results from the numerical analysis of beam structure made up of beams with open cross-section and HSS will be presented and discussed. The obtained results will be verified by means of commercial finite element program and compared with the results obtained by other researchers.

2 DERIVATION OF THE FINITE ELEMENT EQUATIONS

Fig. 1 shows a prismatic beam of length *L*, with *i* as the first node and *k* as the end node. Arbitrary cross-sectional characteristics are described by the cross-sectional area *A,* the torsion constant I_T, the secondary torsion constant I_{Ts} and the warping constant I_ω. Material properties include Young's modulus *E*, and the shear modulus *G*. The state variables $\vartheta(x), \vartheta'_M(x), M_T(x), M_{Ts}, M_\omega(x)$ are the twist angle, the warping part of the first derivative of the twist angle, the torsional moment, secondary torsional moment and the bimoment (warping moment) at position *x*, respectively. The primary torsional moment is $M_{Tp}(x) = M_T(x) - M_{Ts}(x)$. Their values at the first beam node are denoted by index *i*. The last column in the transfer matrices (see (1) and (2), respectively), represents the contribution of distributed external loads, acting on the beam, to the state variables.
The analogy between the second-order beam theory (including the effect of shear deformations and axial tension) and non-uniform torsion theory (including the effect of secondary torsional moment deformation effect) allowes derivation of the transfer relation for the M_{Ts}-formulation (the secondary torsional moment M_{Ts} is analogical to the shear forces; see Fig. 1a and (1)) and M_T-formulation (the torsional moment M_T is analogical to the transversal force: Fig. 1b and expression (1)) [3]:

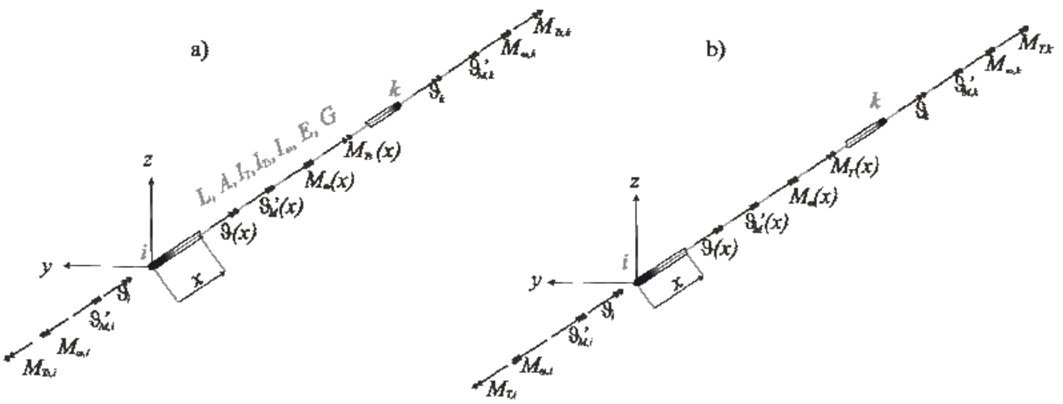

Figure 1: Static and kinematic variables: a) M_{Ts} - formulation; b) M_T - formulation

The functions $b_j(x)$ for $j \in \langle 0,3 \rangle$ are the transfer functions. They are given in [3]: $b_0(x) = \cosh(fx)$, $b_1(x) = \dfrac{\sinh(fx)}{f}$, and $b_j(x) = \dfrac{b_{j-2}(x) - a_{j-2}(x)}{K}$ for $j \geq 2$. The parameters *K*, f, κ, a_0, and a_j are defined as $K = \kappa \dfrac{GI_T}{EI_\omega}$, $f = \sqrt{K}$, $\kappa = \left(1 + \dfrac{I_T}{I_{Ts}}\right)^{-1}$, $a_0(x) = 1$, and $a_j(x) = \dfrac{x^j}{j!}$ for $j \geq 1$, respectively.

$$\begin{bmatrix} \vartheta(x) \\ \vartheta'_M(x) \\ M_\omega(x) \\ M_T(x) \\ 1 \end{bmatrix} = \begin{bmatrix} 1 & \kappa b_1(x) & -\kappa\dfrac{b_2(x)}{EI_\omega} & -\kappa\left(\dfrac{b_3(x)}{EI_\omega} - \dfrac{b_1(x)}{GI_{Ts}}\right) & \vartheta^L \\ 0 & b_0(x) & -\dfrac{b_1(x)}{EI_\omega} & -\kappa\dfrac{b_2(x)}{EI_\omega} & \vartheta_M^{'L} \\ 0 & \kappa GI_T b_1(x) & b_0(x) & \kappa b_1(x) & M_\omega^L \\ 0 & 0 & 0 & 1 & M_T^L \\ 0 & 0 & 0 & 0 & 1 \end{bmatrix} \cdot \begin{bmatrix} \vartheta_i \\ \vartheta'_{M,i} \\ M_{\omega,i} \\ M_{T,i} \\ 1 \end{bmatrix} \tag{1}$$

The transfer functions $b_j(x)$, calculated at $x=L$ are called transfer constants they are denoted b_j, i.e. $b_j = b_j(x = L)$. In the following consideration the M_T - formulation will be used which is a more suitable for the finite element derivation. Setting $x = L$ in (2), the state variables at node *k* we obtained as:

$$\begin{bmatrix} \vartheta_k \\ \vartheta'_{Mk} \\ M_{\omega,k} \\ M_{T,k} \\ 1 \end{bmatrix} = \begin{bmatrix} 1 & \kappa b_1 & -\kappa\dfrac{b_2}{EI_\omega} & -\kappa\left(\dfrac{b_3}{EI_\omega} - \dfrac{b_1}{GI_{Ts}}\right) & \vartheta^L \\ 0 & b_0 & -\dfrac{b_1}{EI_\omega} & -\kappa\dfrac{b_2}{EI_\omega} & \vartheta_M^{'L} \\ 0 & \kappa GI_T b_1 & b_0 & \kappa b_1 & M_\omega^L \\ 0 & 0 & 0 & 1 & M_T^L \\ 0 & 0 & 0 & 0 & 1 \end{bmatrix} \cdot \begin{bmatrix} \vartheta_i \\ \vartheta'_{M,i} \\ M_{\omega,i} \\ M_{T,i} \\ 1 \end{bmatrix} \tag{2}$$

The calculation of the hyperbolic functions in $b_j(x)$ may fail if the stiffness ratio of the beam element $\varepsilon_T = L\sqrt{\dfrac{GI_T}{EI_\omega}}$ is greater then 10. In such a case, L must be reduced until in order to satisfy condition ε_T<10.

The effect of the secondary torsional moment is considered by means of constant $\kappa = \left(1 + \dfrac{I_T}{I_{Ts}}\right)^{-1}$ and the transfer constants b_j, $j \in \langle 0,3 \rangle$. If this effect is disregarded, $\kappa = 1$. This is usually done for the case of beams with open sections where the influence of the secondary torsion moment is insignificant. In the contrary, for HSS beams this effect must be considered, as was previously shown in [3] and [11]. Since the linear first-order beam theory is used, the transfer relations (1) and (2) for torsion are not coupled with transverse bending.

The expression for the secondary torsion constant I_{Ts} depends on the chosen type of the cross-section. It can be found e.g. in [8] and [12]. The local stffness matrix of the rode subjected to non-uniform torsion was derived in [15] by means the transfer relations (2). It will now be implemented into the 3D Timoshenko beam finite element stifness matrix.

Fig. 2 shows a doubly symmetric prismatic beam element of length L^e, with the two nodes *i* and *k*, and with appropriate geometry, static and kinematic variables, and material properties: A [m^2] is the cross-sectional area; I_y [m^4] and I_z [m^4] are the quadratic area moments of inertia; I_T [m^4] is the torsion constant; I_ω [m^6] is the warping constant, I_{Ts} [m^4] is the secondary torsion constant; E is Young's modulus; G is the shear modulus. In order to include warping, an additional degree of freedom is added to the classical nodal variables at each node point. As mentioned previously, the warping part of the first derivative of the twist angle, ϑ'_M, is considered as this degree of freedom [15]. This is advantageous for formulating boundary conditions. If the effect of the secondary torsional moment deformation is not considered: $\vartheta'_M(x) \equiv \vartheta'(x)$. The nodal displacement vector in the local coordinate system, as shown in Fig. 2, is given as

$$\{u^e\}^T = \{u_i \;\; v_i \;\; w_i \;\; \vartheta_{xi} \;\; \vartheta_{yi} \;\; \vartheta_{zi} \;\; \vartheta'_{Mi} \;\; u_k \;\; v_k \;\; w_k \;\; \vartheta_{xk} \;\; \vartheta_{yk} \;\; \vartheta_{zk} \;\; \vartheta'_{Mk}\} \tag{3}$$

where u, v, w and ϑ_x, ϑ_y, ϑ_z are the classic degrees of freedom of the node points *i* and *k*. The respective nodal load vector is given as

$$\{F^e\}^T = \{N_i \;\; T_{yi} \;\; T_{zi} \;\; M_{xi} \;\; M_{yi} \;\; M_{zi} \;\; M_{\omega i} \;\; N_k \;\; T_{yk} \;\; T_{zk} \;\; M_{xk} \;\; M_{yk} \;\; M_{zk} \;\; M_{\omega k}\} \tag{4}$$

where $M_{xi} = M_{Ti}$ and $M_{xk} = M_{Tk}$ are the torsional moments, $M_{\omega i}$ and $M_{\omega k}$ are the bimoments, $M_{yi}, M_{yk}, M_{zi}, M_{zk}$ are the bending moments, N_i and N_k are the axial forces and $T_{yi}, T_{yk}, T_{zi}, T_{zk}$ are the shear forces.

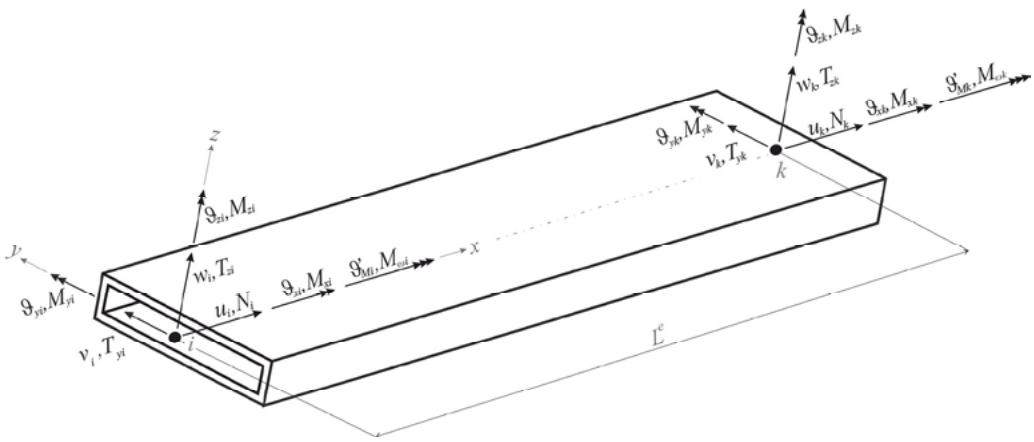

Figure 2: W-beam finite element, considering non-uniform torsion, in the local coordinate system

Enhancing the classical Timoshenko beam finite element representation by the stiffness matrix for non-uniform torsion of straight beams [15] gives the local equations for the 3D Timoshenko beam finite element with warping (W-beam), (5).

$$\{F^e\} = [K^{le}]\{u^e\} \tag{5}$$

The effect of the secondary torsional moment and of the shear force on the deformations is already included in the local finite element stiffness matrix $\left[K^{le}\right]$, which is given as:

$$
\left[K^{le}\right]=\begin{bmatrix}
k_{1,1} & 0 & 0 & 0 & 0 & 0 & 0 & k_{1,8} & 0 & 0 & 0 & 0 & 0 & 0 \\
 & k_{2,2} & 0 & 0 & 0 & k_{2,6} & 0 & 0 & k_{2,9} & 0 & 0 & 0 & k_{2,13} & 0 \\
 & & k_{3,3} & 0 & k_{3,5} & & 0 & 0 & 0 & k_{3,10} & 0 & k_{3,12} & 0 & 0 \\
 & & & k_{4,4} & 0 & 0 & k_{4,7} & 0 & 0 & 0 & k_{4,11} & 0 & 0 & k_{4,14} \\
 & & & & k_{5,5} & 0 & 0 & 0 & 0 & k_{5,10} & 0 & k_{5,12} & 0 & 0 \\
 & S & & & & k_{6,6} & 0 & 0 & k_{6,9} & 0 & 0 & 0 & k_{6,13} & 0 \\
 & & Y & & & & k_{7,7} & 0 & 0 & 0 & k_{7,11} & 0 & 0 & k_{7,14} \\
 & & & M & & & & k_{8,8} & 0 & 0 & 0 & 0 & 0 & 0 \\
 & & & & M & & & & k_{9,9} & 0 & 0 & 0 & k_{9,13} & 0 \\
 & & & & & E & & & & k_{10,10} & 0 & k_{10,12} & 0 & 0 \\
 & & & & & & T & & & & k_{11,11} & 0 & 0 & k_{11,14} \\
 & & & & & & & R & & & & k_{12,12} & 0 & 0 \\
 & & & & & & & & I & & & & k_{13,13} & 0 \\
 & & & & & & & & & C & & & & k_{14,14}
\end{bmatrix} \tag{6}
$$

If we denote the torsional stiffness terms in (2) as $k_1 = \dfrac{b_1}{EI_\omega}$, $k_2 = \dfrac{b_2}{EI_\omega}$ and $k_3 = \left(\dfrac{b_3}{EI_\omega} - \dfrac{b_1}{GI_{Ts}}\right)$ the non-uniform torsion stiffness terms in (6) are given as $k_{4,4} = k_{11,11} = -k_{4,11} = \dfrac{ck_1}{\kappa k_2}$, $k_{4,7} = k_{4,14} = -k_{7,11} = -k_{11,14} = -c = \dfrac{-k_2}{\kappa k_2^2 - k_1 k_3}$, $k_{7,7} = k_{14,14} = c\left(\kappa b_1 - b_0 k_2 / k_2\right)$ and $k_{7,14} = ck_3 / k_2$.

The axial and flexural stiffness terms in (6) are obtained as $k_{1,1} = k_{8,8} = -k_{1,8} = \dfrac{EA}{L}$, $k_{2,2} = = k_{9,9} = -k_{2,9} = 12\dfrac{EI_z}{L^3}\left(1+12\rho_z\right)$, $k_{2,6} = k_{2,13} = 6\dfrac{EI_z}{L^2}\left(1+12\rho_z\right)$,

$$k_{3,3} = k_{10,10} = -k_{3,10} = 12\frac{EI_y}{L^3}\left(1+12\rho_y\right), \qquad k_{3,5} = -k_{3,12} = -k_{10,12} = k_{10,12} = -6\frac{EI_y}{L^2}\left(1+12\rho_y\right),$$

$$k_{5,5} = k_{12,12} = \frac{EI_y}{L}\left(1+\frac{3}{1+12\rho_y}\right), k_{6,6} = k_{13,13} = \frac{EI_z}{L}\left(1+\frac{3}{1+12\rho_z}\right),$$

$$k_{6,9} = k_{9,13} = -6\frac{EI_z}{L^2}\left(1+12\rho_z\right),\ k_{6,13} = \frac{EI_z}{L}\left(\frac{3}{1+12\rho_z}-1\right), \text{ and } k_{5,12} = \frac{EI_y}{L}\left(\frac{3}{1+12\rho_y}-1\right).$$

The parameters $\rho_y = \frac{EI_y}{L^2 k_y^s GA}$ and $\rho_z = \frac{EI_z}{L^2 k_z^s GA}$ are stiffness ratios with the shear correction factors k_y^s and k_z^s ($k_y^s = k_z^s = 5/6$ for the rectangular cross-sections, etc...).
The secondary and the primary torsional moments at the node points' are given as [3]

$$M_{Tsi} = \kappa\left(M_{Ti} - GI_T \vartheta'_{Mi}\right);\ M_{Tsk} = \kappa\left(M_{Tk} - GI_T \vartheta'_{Mk}\right) \tag{7}$$

and

$$M_{Tpi} = M_{Ti} - M_{Tsi};\ M_{Tpk} = M_{Tk} - M_{Tsk} \tag{8}$$

The expressions for calculation of the shear and normal stress calculation depend on the type of the cross-sectional area. This problem was described in detail in [10]. These expressions will be used for calculation of the stresses in the numerical investigation.
The element stiffness matrix (6), the displacement vector (3) and the load vector (4) have to be transformed from the local to a global coordinate system. The global equation system of the whole beam structure will be obtained in a usual way. After its solution, the local distribution of the internal forces and displacements can be calculated. The local rotation angles and torsional moments of non-uniform torsion can be calculated via the local transfer relations (1). A computer code has been written in the Mathematica software [20] in which the above-presented new 3D Timoshenko beam finite element (W-beam) has been implemented.

3 NUMERICAL INVESTIGATION

The beam deflection of the structure and the effect of secondary torsion moment are investigated. The steel frame (Fig. 3), which was analyzed in [21] by boundary and finite element method, comprising of two different cross-sections (IPE-400 and RHS-400x200x12), is loaded by a transverse force-couple F = 50 kN. The radius of the semicircular part is equal to 5 m. Young's modulus E and Poisson ratio ν are given as 2.1x10^5 MPa and 0.3, respectively. The cross-sectional characteristics in Table 2, based on the chosen dimensions for the IPE-400 (h = 386.5 mm, b = 200 mm, t_w = 13.5 mm and t_f = 8.6 mm) and RHS-400x200x12 (h = 388 mm, b = 188 mm and t_w = t_f=12 mm), were obtained from the general expressions in Table 1.

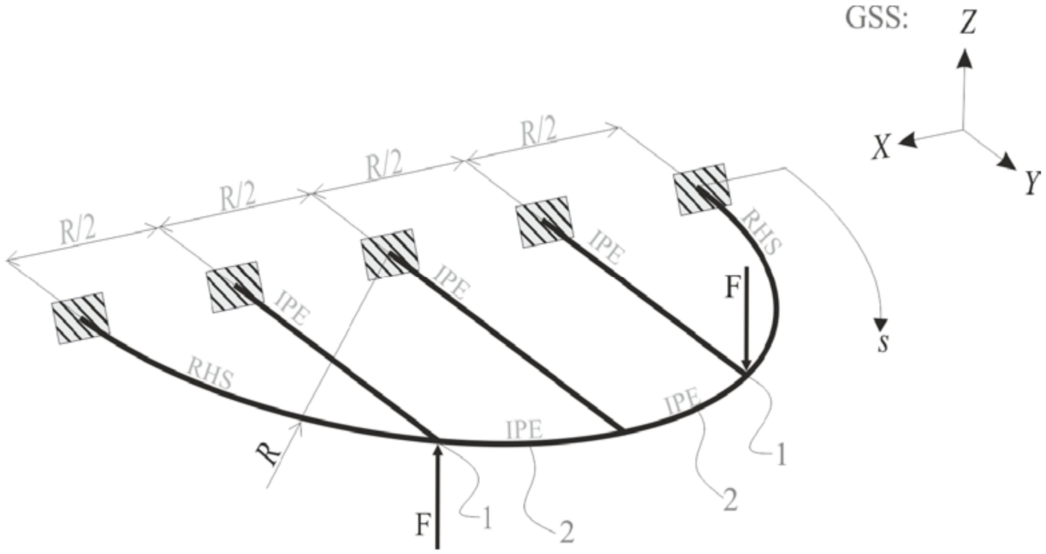

Figure 3: Steel frame loaded by a transverse force-couple and global coordinate system X,Y,Z

		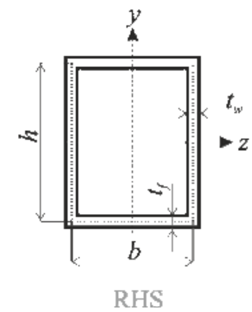 RHS	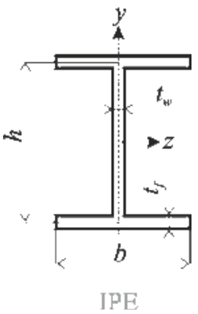 IPE
cross-sectional parameters	γ	$h/t_w + b/t_f$	-
	A	$2(ht_w + bt_f)$	$t_w h + 2t_f b$
	ω_R	$\frac{hb}{4} \cdot \frac{ht_f - bt_w}{ht_f + bt_w}$	$\frac{hb}{4}$
	I_ω	$\omega_R^2 \frac{A}{3}$	$\omega_R^2 \frac{2t_f b}{3}$
	I_T	$\frac{2(hb)^2}{\gamma}$	$\frac{t_w^3 h + 2t_f^3 b}{3}$
	I_{Ts}^{-1}	$\frac{\frac{(Ahb)^2}{hbt_w t_f} + \frac{(h^2+b^2)^2}{1,5}}{20\gamma I_\omega A}$	$\frac{5t_f bh^2}{12}$

Table 1: Expressions for the cross-sectional characteristics calculation

		RHS-400x200x12	IPE-400
cross-sectional characteristics	A [m^2]	1.382×10^{-3}	8.184×10^{-3}
	ω_R [m^2]	6.332×10^{-3}	1.933×10^{-2}
	I_ω [m^6]	1.848×10^{-7}	4.990×10^{-7}
	I_z [m^4]	2.803×10^{-4}	2.314×10^{-4}
	I_T [m^4]	2.293×10^{-7}	5.181×10^{-7}
	I_{Ts} [m^4]	2.671×10^{-5}	3.209×10^{-3}

Table 2: Cross-sectional characteristics

Information about the density of the mesh, consisting of W-beam elements is given in Fig. 4. The mesh consists of 52 elements. The analysis was performed for two different assumptions:

a) both, the effect of the shear-force and of the secondary torsion moment on the deformations was considered,
b) only the effect of the secondary torsion moment on the deformations was taken into account.

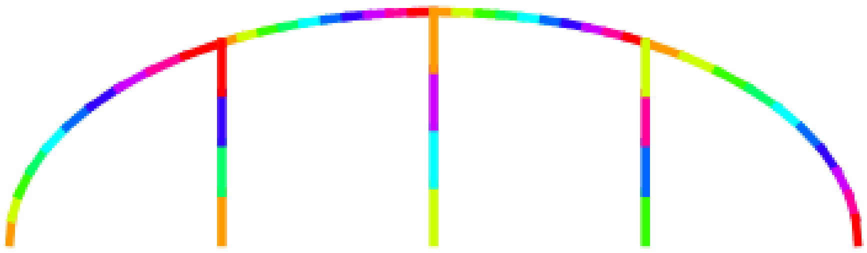

Figure 4: Mesh of W-beam finite elements

The deflection (displacement in global z direction) of the frame for the case of consideration of the effect of the shear force and the secondary torsion moment on the deformation is shown in Fig. 5. The deformation of the frame is anti-symmetric. The maximum deflection occurs at the load points. It is given as $u_{z,max}$ = 7.446 mm. If we neglect the deformations due to shear forces, the maximum deflection decreases to 7.291 mm.
The distribution of the bimoment along the curved part of the structure is displayed in Fig. 6, there s denotes the arc-length. Important results are shown in Table 3. They are compared with results published in [21].

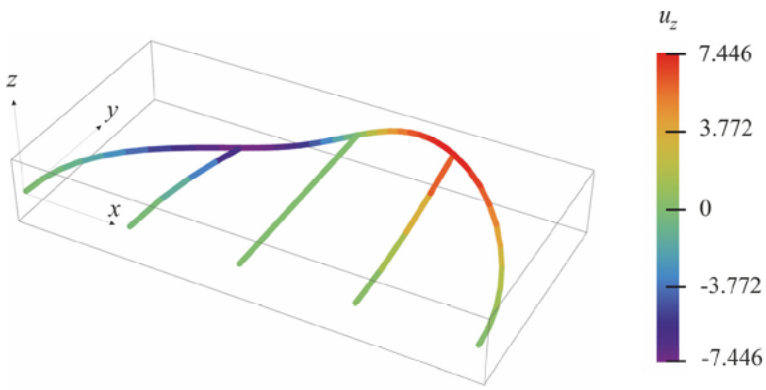

Figure 5: Deflection of the frame considering the influence of the shear force and the secondary torsion moment on the deformation, calculated with W-beam finite elements

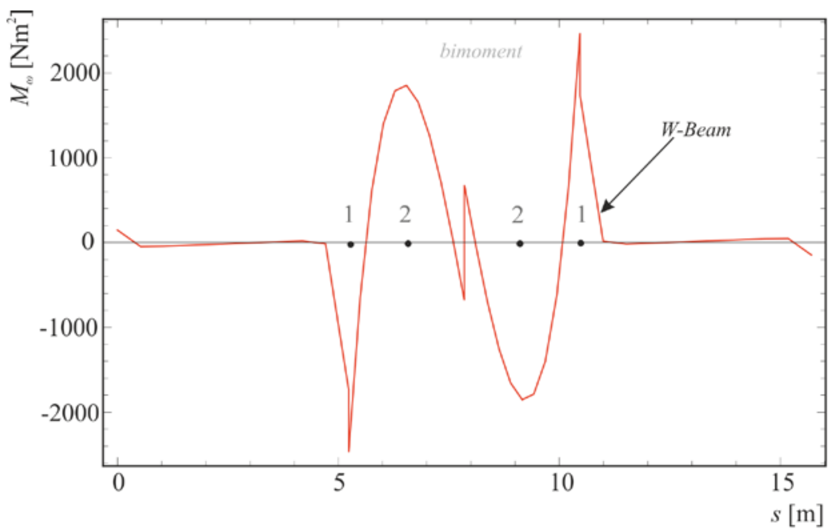

Figure 6: Distribution of the bimoment along the curved part of the structure

	W-beam	W-beam*	BEM [21]	shell FE [21]
ordinate position 1: s ~ 5.24 m				
M_ω [Nm^2]	2471.9	2477.6	2481.9	-
$u_{z,max}$ [mm]	7.446	7.509	7.513	7.582
ordinate position 2: s ~ 6.29 m				
M_ω [Nm^2]	1853.2	1816.8	1821.9	-

Table 3: Bimoment M_ω and deflection u_z , obtained numerically by means of the proposed W-beam, boundary element-beam (BEM) and by shell finite element (FE) [21]. W-beam* uses cross-sectional properties calculated by the BEM [21]

Incorrect results are obtained if the effect of the secondary torsion moment on the deformations is neglected. For κ = 1, the transfer constants become very large making solution results random numbers as was also stated in [15].

As expected, the maximum bimoment, $M_{\omega,max}$ = 2471.9 Nm^2 , occurs at the two load points, where a step change in $M_\omega(s)$ can be seen. In comparison with BEM and shell elements results our proposed 3D beam gives satisfactory results at all important positions.

It is worthy of note that there is a difference in some cross-sectional parameters obtained by the BEM and the FEM which affects the overall stresses and displacements. The most difference was found to occur for the warping constant. The W-beam* in Table 1 uses the following values values $I_{Ts,IPE}$ = 166.611×10^{-6} m^4, $I_{\omega,IPE}$ = 4.835×10^{-7} m^6, $I_{Ts,RHS}$ = 26.701×10^{-6} m^4 and $I_{\omega,RHS}$ = 2.056×10^{-7} m^6 obtained by the BEM [21]. Their impact on the bimoment and the deflection is clearly prominent.

4 CONCLUSIONS

This paper deals with the derivation of a new 3D Timoshenko beam (W-beam) finite element with doubly-symmetric cross-section considering the non-uniform torsion. The analogy between the 2nd-order beam theory (with axial tension) and torsion with warping (with the effect of the secondary torsional moment on the deformations) and the transfer relations were used for derivation of the torsional terms of the stiffness matrix of the beam finite element. The influence of the secondary torsional moment on the deformations must be considered especially in non-uniform torsion of HSSs. This fact has been verified by measurements carried out via author's measurement device designed especially for this purpose [18]. The new finite element can be used for analyses of non-uniform torsion of spatial beam structures consisting of members with open as well as closed cross-sections. The majority of the obtained results agree very well with theoretical predictions. However, the results from numerical analysis of non-uniform torsion of beam with closed cross-sections, as carried out using the Beam188 finite element of commercial software [6], differ significantly from measurement results. The significance of the inclusion of warping in the analysis of both open and closed cross-sections was confirmed numerically and experimentally. This is in contradiction with the widely used Eurocodes [4], [5]. New results should lead to modifications of current Eurocodes.

Acknowledgement:
This research on which the paper is based was supported by the APVV Agency (project No.: SK-AT-0001), the Grant Agency VEGA (grant No.: 1/0534/12) and the and by the project CRISIS ITMS 26240220060. This support is gratefully acknowledged.

REFERENCES

[1] Vlasov, V.Z. *Thin-walled elastic beams*. National Science Foundation, Washington, (1961).

[2] Roik, K. and Sedlacek, G. Theorie der Wölbkrafttorsion unter Berücksichtigung der sekundären Schubverformungen - Analogiebetrachtung zur Berechnung des querbelasteten Zugstabes. *Stahlbau* **35**, 43, (1966).

[3] Rubin, H. Wölbkrafttorsion von Durchlaufträgern mit konstantem Querschnitt unter Berücksichtigung sekundärer Schubverformung. *Stahlbau* **74**, Heft 11, 826, (2005).

[4] EN 1993 - Eurocode 3: Design of steel structures, European Committee for Standardization (CEN). (2004).

[5] EN 1999 - Eurocode 9: Design of aluminium structures, European Committee for Standardization (CEN). (2007).

[6] ANSYS Swanson Analysis System, Inc., 201 Johnson Road, Houston, PA 15342/1300, USA, (2013).

[7] RSTAB, Ingenieur - Software Dlubal GmbH, Tiefenbach, (2006).

[8] Sapountzakis, E.J. and Mokos, V.G. 3-D beam element of composite cross-section including warping and shear deformation effect. *Computers and Structures* **85**, 102, (2007).

[9] Mokos, V.G. and Sapountzakis, E.J. 3-D beam element of variable composite cross-section including warping effect. *Acta Mechanica*, **171** (3-4), 703, (2004).

[10] Rubin, H. Torsions-Querschnittswerte für rechteckige Hohlprofile nach EN 10210-2: 2006. *Stahlbau* **76**, Heft 1, (2007).

[11] Rubin, H. Zur Wölbkrafttorsion geschlossener Querschnitte und ihrer Irrtümer – Grundlagen. 29. Stahlbauseminar, Band **140**, ISSN: 1615-4266, (2007).

[12] Rubin, H. and Aminbaghai, M. Wölbkrafttorsion bei veränderlichem, offenem Querschnitt - hat die Biegezugstabanalogie noch Gültigkeit?, *Stahlbau*, **76**, 747, (2007).

[13] Rubin, H., Aminbaghai, M. and Weier, H. IQ-100. The civil engineering structures program, TU Vienna, Bautabellen für Ingenieure, Werner Verlag, 17. Auflage, (2006).

[14] Rubin, H. *Baustatik 2*. Manuskript der Vorlesung. Institute of Structural Analysis", Vienna University of Technology, (2007).

[15] Murin, J. and Kutis, V. An effective finite element for torsion of constant cross-sections including warping with secondary torsion moment deformation effect, *Engineering Structures*, ISSN 0141-0296, Vol. **30**, Iss. 10, 2716-2723, (2008).

[16] Mokos, V.G. and Sapountzakis, E.J. Secondary torsional moment deformation effect by BEM, *International Journal of Mechanical Science*. IJMS-10323R1, (2011).

[17] Tsipiras, V.J. and Sapountzakis, E.J. Secondary torsional moment deformation effect in inelastic non-uniform torsion of bars of doubly symmetric cross section by BEM, *International Journal of Non-Linear Mechanics*. **47**, 68 - 84, (2012).

[18] Murin, J., Sedlar, T., Kalas, A. and Kralovic, V. A device for measurement of non-uniform torsion of the thin-walled cross-sections, Patent 6017 Slovak Republic, (2012) (In Slovak).

[19] Rubin, H. "Vorlesung: *BAUSTATIK 2*. Grundlegende Formeln der Theorie II. Ordnung", Institut für Baustatik TU Wien, (2009).

[20] Wolfram Research, Inc., Mathematica, Version 8.0, Champaign, IL, USA (2010).

[21] Mokos, V.G. and Sapountzakis, E.J. A three-dimensional beam including torsional warping and shear deformation effects arising from shear forces and secondary torsional moments, Proceedings of the Thirteenth International Conference of Civil, Structural and Environmental Engineering Computing, (2011).